

Periodic Mesoporous Organosilica-Based Nanocomposite Hydrogels for Enhanced Cell Adhesion in 3D Hydrogel Network

Nermin Seda Kehr

Physikalisches Institut and Center for Soft Nanoscience, Westfälische Wilhelms-Universität Münster, Busse-Peus-Strasse 10, 48149 Münster, Germany

*Corresponding Author Received: August 4, 2019 E-mail: seda@uni.muenster.de Accepted: October 25, 2019

ABSTRACT

The chemical functionalization of nanomaterials with bioactive molecules has been used extensively to generate functional biomaterials for tissue engineering, drug delivery, and wound healing applications and to study the cell-material interactions. In this context, this study describes the synthesis of PEG and PMO based nanocomposite hydrogels as new 3D biomaterial and the impact of surface functionalization of PMOs on cell adhesion in 3D network of PEG hydrogel. The results show that the affinity of cells to the PEG hydrogel can be controlled by using biomolecule functionalized PMO particles. The observed results are attributed to the large nanoscale surface area of PMOs and the cell adhesive character of the used bioactive molecules on the surface of PMOs.

Keywords: Nanocomposite hydrogel, cell adhesion, periodic mesoporous organosilica, poly(ethylene glycol)

INTRODUCTION

Nanocomposite (NC) polymer hydrogels[1,2] or in other words, organic-inorganic hybrid nanocomposites are an important class of soft hybrid materials. NC hydrogels are produced by chemical or physical crosslinking of organic polymers in water in the presence of nanometerials (NMs) such as clays, silica nanoparticles, magnetic nanoparticles or carbonnanotubes[3]. NC hydrogels show extraordinary mechanical strength and swelling/deswelling properties due to the reinforcement of the polymer matrix with NMs[3]. The incorporation of NMs into hydrogel networks not only improves the mechanical properties, but also imparts superior biological properties of NC hydrogels[3].

Up to date, different inorganic NMs and polymers have been used for the preparation of NC hydrogels. For example, different kinds of clays (e.g., hectorite, montmorillonite) and their modified forms (e.g., by fluorination),[4] other minerals such as polyhedral oligomeric silsesquioxane,[5] rigid polysiloxane,[6] fibrillar attapulgite[7] and hydrotalcite[8] have been used with selected polymers such as N-isopropylacryamide and N,N-dimethylacrylamide[9] to form NCs. Besides clays, silica particles have been used to generate NC hydrogels. For example, Van Durme et al.[10] have reported the polymerizing N-isopropylacrylamide in the presence of silica particles enhanced the elastic properties and the swelling/deswelling kinetics of the hydrogel network. Similarly, specific interactions between silica nanoparticles and polymer side-chains grafted onto a non-adsorbing poly(acrylamide) backbone have been described by Hourdet et al.[8,11]. The same group is then reported the "self crosslinked" hydrogels with improved mechanical properties by introducing silica nanoparticles that interact strongly with polymer chains. In addition, to clays and silica nanoparticles, other nanoparticles such as gold, silver, as well as metal alloys, salts, metal-derived quantum dots (2-100 nm) and magnetic nanoparticles have been mixed with or synthesized within a hydrogel matrix to reach NC hydrogels with novel properties[12].

Most of these studies are limited to use of non-functionalized nanomaterials. Therefore, later, Kehr et al, demonstrated the fabrication of new NC hydrogels based on functionalized nanoparticles. In these studies, periodic mesoporous organosilicas (PMOs) were functionalized with different bioactive molecules and embedded into the alginate hydrogel networks to study the impact of nanoparticle functionalization on cell behavior[13-19]. Despite the exiting results of these NC hydrogels. They are still restricted to the used hydrogel, alginate (a natural hydrogel), for the preparation of NC hydrogels.

In this respect, in this study, the synthetic polymer, poly(ethylene glycol) (PEG) was used to generate functional NC hydrogels for cell-material interaction studies. PEG is a highly biocompatible synthetic polymer, extensively used in the biomedical field due to its less toxicity, non-immunogenicity and biocompatibility. Furthermore, in order to generate PEG-based NC hydrogel, biomolecule functionalized PMOs were used in this work. PMOs are excellent candidates as porous nanoparticles for biocompatible NC hydrogel formation due to its unique properties. PMOs[20-22], which are class of functional organic-inorganic hybrid mesoporous silica nanoparticles were first described in 1999 by three independent research groups [23-25]. In contrast to other hybrid inorganic/organic silica based materials where organic units are implemented onto silica framework via post-synthetic treatment the organic functions are directly and homogeneously incorporated into the pore wall network of PMOs by two covalent bonds. PMOs provide a high ordering of mesoporous, high specific surface area, narrow pore size distributions, and high thermal and mechanical stability. Due to these interesting properties of PMOs, significant efforts have been devoted to the preparation and study of these materials with different bridged organic groups, pore structures and morphologies, as well their potential applications in different fields such as catalysis, adsorption, chromatography, protein separation, and drug release systems[20-22].

MATERIALS AND METHODS

Materials: Hexadecyltrimethylammonium bromide (CTAB, 98%), 1,2-bis(trimethoxysilyl)ethane (BTME, 96%), 3-aminopropyltrimethoxysilane (APTES, 99%), arginine-glycine-aspartic acid (RGD), N-hydroxy-succinimide (NHS), poly(ethylene glycol) (PEG) , and α -cyclodextrin (CD) were purchased from Sigma-Aldrich. 1-Ethyl-3-(3-dimethylaminopropyl)carbodiimid (EDC) was obtained from ABCR. Ethanol (absolute for analysis), ammonia solution (32%, pure) and hydrochloric acid (32%, for analysis), were purchased from Merck (stored over molecular sieves, puriss., H₂O 0.005%). 4',6-diamidino-2-phenylindole-6-carboxamidine (DAPI) was purchased by AppliChem-Bio-Chemica and Life Technologies GmbH. The cell medium (supplemented with 200 µg/mL Penicillin/Streptomycin, 200 μg/mL Gentamycin) and 10% (v/v) fetal bovine serum (FBS) were obtained from Biochrom, Germany.

Synthesis of PMO-NH₂: 484.5 mg of CTAB was dissolved in 88 mL of $\rm H_2O$, 33 mL of ethanol, and a 28 wt% ammonia (0.075 g) solution. The reaction mixture was stirred at room temperature for 1 h before the addition of BTME (1.27 g) and APTES (0.26 g). The above reaction mixture was continuously stirred for an additional 72 h at room temperature. The CTAB mesoporous template was removed by stirring the sample in ethanol (50 mL) with a 36 wt% aqueous solution of HCl (1.5 g) at 50 °C for 6 h. The resulting solid (PMO-NH₂) was recovered by centrifugation, washed with ethanol and acetone several times, and dried at 60 °C under vacuum.

Synthesis of PMO-RGD: A solution of 0.4 mM RGD peptide, 3.0 mM EDC, and 6.0 mM NHS in 1 mL DMSO was added dropwise to a suspension of the PMO-NH₂ (20 mg) in 1 mL DMSO. The reaction mixture was stirred for 16 h at room temperature. Subsequently the suspension was centrifuged 10 min at 4400 rpm and the isolated solid was washed with DMSO x 2 and ethanol x 2. Finally, the solid (PMO-RGD) was dried at room temperature.

Synthesis of PEG/CD hydrogel: PEG/CD hydrogel was prepared by sonication of PEG/ α -CD aqueous solution (170/150 mg/ml) for 1 min.

Synthesis of PMO-PEG/CD NC hydrogels: PMO-PEG/CD NC hydrogels were prepared by mixing PEG/ α -CD aqueous solution (170/150 mg/ml) and PMO-NH $_2$ or PMO-RGD aqueous suspension (1 mg/ml). The resulting suspension was then sonicated for 1 min to obtain PMO-NH $_2$ -PEG/CD or PMO-RGD-PEG/CD.

Cell Experiments in PEG/CD, PMO-NH₂-PEG/CD or PMO-RGD-PEG/CD: The cells were carefully thawed and resuspended in their specific medium. Cells were seeded (50.000 cells) into the hydrogels and incubated for 1 day and 5 days of incubation at 37 °C and 5% CO₂ in an incubator. After incubation time, to remove non-adhered cells the hydrogels were washed twice with media. Then hydrogels were treated with trypsin for 10 min incubation time and dissolved by gently mixing with 1 mL PBS⁺⁺ (supplemented with 0.5 mM MgCl₂, 0.9 mM CaCl₂). Afterwards, the number of viable cells (0.4% Trypan diluted in MilliQ) was detected by using automatic cell counter (Biorad).

For fluorescence microscopy images, cell nucleus in PEG/CD, PMO-NH₂-PEG/CD or PMO-RGD-PEG/CD were stained with 4',6-diamidino-2-phenylindole carboxamidine (DAPI) and washed twice with PBS.

Characterization: The morphology of the PMOs was investigated using a Zeiss 1540 EsB dual beam focused ion beam/field emission SEM with a working distance of 8 or

9 mm and an electronic high tension (EHT) of 3 kV. Fluorescence microscopy was carried out with Brunel SP300-FL fluorescence microscopy. ATR-IR spectra were carried out with Golden Gate ATR Accessory. Zeta potential measurements and DSL were done with Malvern Zetasizer Nano Series. Cells were counted with TC10TM automatic cell counter from Bio-Rad.

RESULTS and DISCUSSIONS

The bioactive molecules functionalized PMOs were synthesized and characterized according to the literature described by us. ¹⁹ Briefly, amino-functionalized PMOs were synthesized (PMO-NH₂) and treated with cell adhesive tripeptide Arg-Gly-Asp (RGD) in the presence of EDC and NHS to obtain PMO-RGD. The obtained PMO-RGD nanometer-scale particles were characterized by scanning electron microscopy (SEM), attenuated total reflection (ATR) IR spectroscopy, and zeta potential measurements.

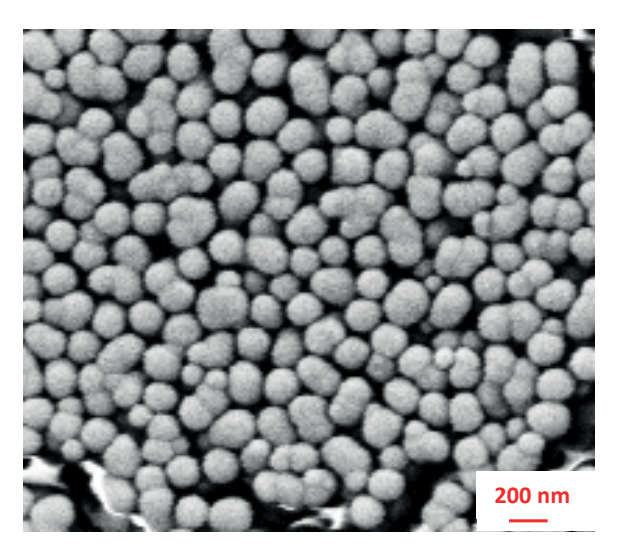


Figure 1. SEM image of PMO-RGD.

The synthesized PMO-RGD particles are uniform and spherical shaped with ca. 171 \pm 27 nm in size (Figure 1). The IR bands of the v(CO) and v(CN) vibrations of the amide bonds of the PMO-RGD confirm the functionalization of PMO-NH $_2$ with the RGD unit. The characteristic IR bands for amide I and amide II absorptions were observed at about 1639 cm $^{-1}$ and 1559 cm $^{-1}$ (Figure 2). While PMO-NH $_2$ shows no corresponding IR bands (Figure 2). Furthermore, the significant increase of the zeta potential from 18 mV (PMO-NH $_2$) to 48 mV (PMO-RGD) at pH 7.2 is another indication of the functionalization of PMO-NH $_2$ with RGD.

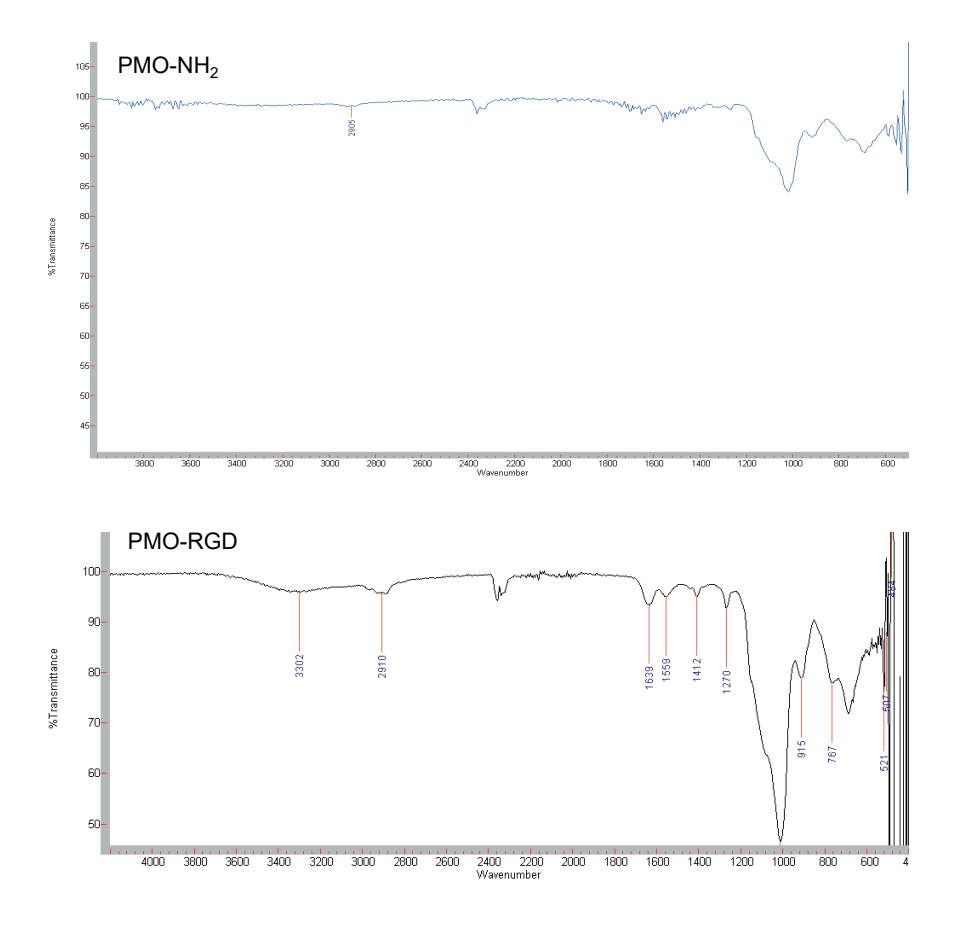


Figure 2. IR spectra of PMO-NH, and PMO-RGD.

NC hydrogels were prepared by the addition of an aqueous solution of PEG and $\alpha\text{-cyclodextrin}$ (CD) to the aqueous suspension of PMO-NH $_2$ or PMO-RGD. NC hydrogels (PMO-NH $_2\text{-PEG/CD}$ and PMO-RGD-PEG/CD) were formed due to the cooperative complexation of CD and PEG

chains. This cooperative interaction initiated the crosslinking of PEG chains with CD and started self-assembly process which caused supramolecular hydrogel formation based on polypseudorotaxane formation like described in the literature [26-27].

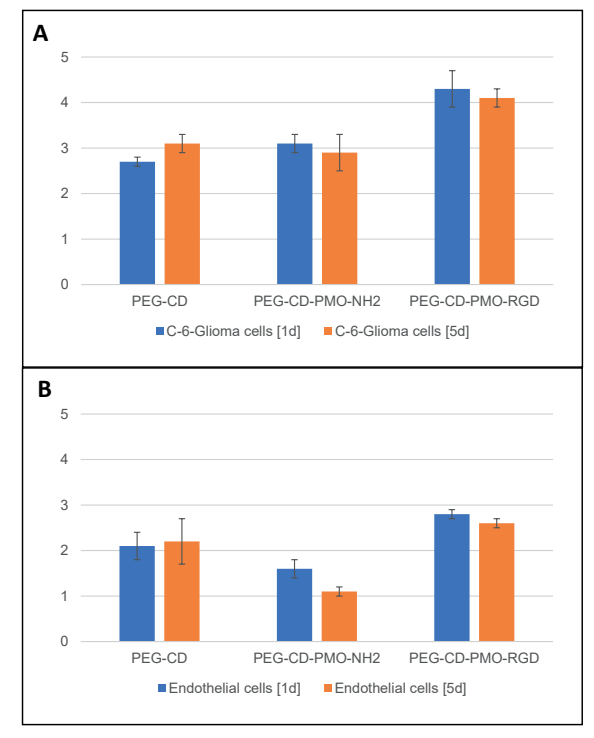


Figure 3. The number of live C-6-Glioma (A) and Endothelial (B) cells after 1 day and 5 days incubation time in PEG/CD, PMO-NH₂-PEG/CD and PMO-RGD-PEG/CD.

Subsequently, cell adhesion experiments were carried out using C-6-Glioma (cell line rat astrocyte glioma cancer cells) and primary porcine brain capillary Endothelial cells (PBCEC). Cells were seeded separately into the PMO-RGD-PEG/CD scaffolds. As control experiments, the same cells were seeded on PEG/CD and PMO-NH₂-PEG/CD, respectively. After 1 day and 5 days incubation time, the adhered cells in the respective NC hydrogels were counted using an automatic cell counter (Figure 3, Table 1). The results showed that C-6-Glioma and Endothelial cells have similar affinities to the respective NC hydrogel scaffolds. The total number of viable cells in PMO-RGD-PEG/CD was higher than that in PMO-NH₂-PEG/CD and PEG/CD scaffolds at 1 day and 5 days incubation time. The extracted amount of viable C-6-Glioma cells in PMO-RGD-PEG/CD was 1.6 and

1.4 times more than that in PEG/CD and PMO-NH₂-PEG/CD, respectively, after 1 day of incubation. While, 0.8 and 1.8 times more Endothelial cells were obtained in PMO-RGD-PEG/CD than that in PEG/CD and PMO-NH₂-PEG/CD, respectively. After an increase of the incubation time (5 days), the difference between the scaffolds becomes less pronounced. While the number of cells in PEG/CD was getting higher, a decrease in the cell number in PMO-NH₂-PEG/CD and PMO-RGD-PEG/CD was observed. However, both cell types still showed higher affinity to PMO-RGD-PEG/CD (C-6-Glioma: 1.3 and 1.4 times more; Endothelial cells: 1.2 and 2.4 times more) than to PEG/CD and PMO-NH₂-PEG/CD, respectively.

able C-6-Glioma cells in PMO-RGD-PEG/CD was 1.6 and **Table 1.** Numbers (x 10⁴) of live C-6-Glioma/Endothelial cells in PEG/CD, PMO-NH₂-PEG/CD and PMO-RGD-PEG/CD at 1 day and 5 days of incubation time.

	PEG-CD	PEG-CD-PMO-NH ₂	PEG-CD-PMO-RGD
C-6-Glioma cells [1d]	2.7 ± 0.1	3.1 ± 0.2	4.3 ± 0.4
C-6-Glioma cells [5d]	3.1 ± 0.2	2.9 ± 0.4	4.1 ± 0.2
Endothelial cells [1d]	2.1 ± 0.3	1.6 ± 0.2	2.8 ± 0.1
Endothelial cells [5d]	2.2 ± 0.5	1.1 ± 0.1	2.6 ± 0.1

These results demonstrate that the cell affinity on biomaterials surfaces can be enhanced by using functionalized nanometer-scale particles. The functionalization of the PMO with cell adhesive short-chain peptide RGD promoted the cell affinity to the matrix of the PMO-PEG/CD hydrogel. The RGD peptide sequence is a crucial adhesive protein in the extracellular matrix (ECM). RGD plays an important role in focal cell adhesion via its bioconjugation to specific integrin molecules (ca. 10-12 nm in size) [28] on cell membrane. Therefore, many cell functions are regulated by biomolecules, which has nanoscale dimensions. In this respect, it is important to conjugate a single molecule of ECM component such as the RGD to nanomaterials to stimulate the integrin distribution across the cell membrane and study the impact of ECM component on cell-material interaction studies.

In addition, the large nanoscale surface area of nanomaterials causes surface roughness on hydrogel surfaces that al-

lows a larger number of contact points between the cell and the material surface, resulting in a more efficient interaction, and therefore, for example in our case, to a better affinity of cells to the PMO-PEG-CD hydrogel.

The reason of less cell affinity to PMO-NH₂-PEG/CD can be attributed to the charged dependent toxicity of PMO-NH₂. The positively charged PMO-NH₂ can stress the negatively charged cell membrane and this can lead to cell injuries and death like described in the literature [29].

Finally, the morphologies of the cells in PEG/CD, PMO-NH₂-PEG/CD and PMO-RGD-PEG/CD were visualized by fluorescence microscopy images (Figure 4). The nucleus of the cells was stained with 4',6-diamidino-2-phenylindole-6-carboxamidine (DAPI, blue). The adhered C-6-Glioma and Endothelial cells have spherical shape morphology and they form agglomerates inside of the hydrogel scaffolds. The spherical shape morphology of cells inside of the hydrogel scaffolds indicates that cell attached on the whole surfaces of the 3D hydrogels.

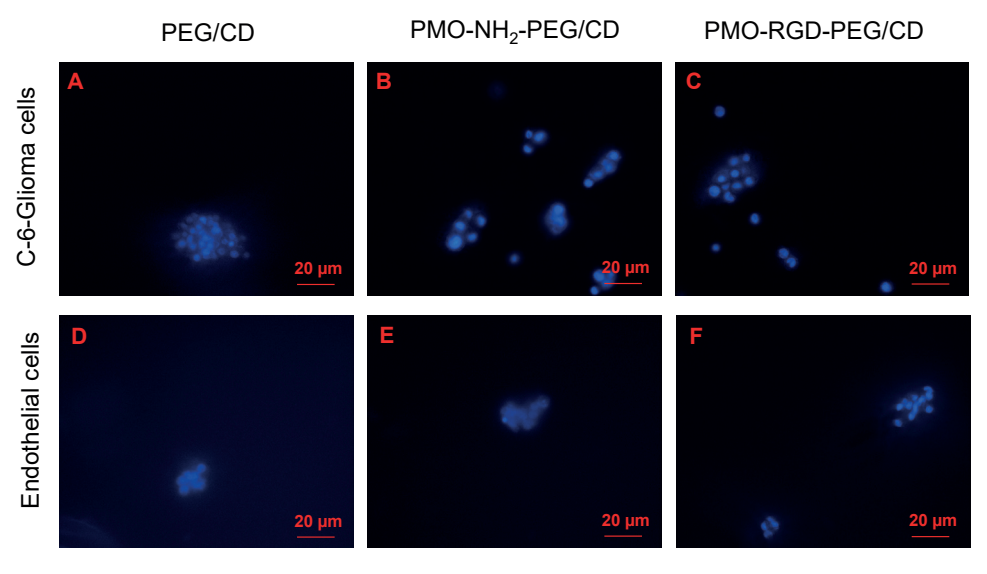


Figure 4. Fluorescence microscopy images of C-6-glioma (A-C) and Endothelial (D-F) cells in PEG/CD (A, D), PMO-NH₂-PEG/CD (D, e) and PMO-RGD-PEG/CD (C, F) (blue: DAPI-stained cells).

CONCLUSION

In conclusion, the preparation of PEG and PMO based NC hydrogels and the effect of biomolecules of the particle surface on the interaction of cells within 3D NC hydrogels were demonstrated. The results showed that the affinity of live cells towards PEG hydrogel was enhanced by using RGD functionalized PMO particles due to the large nanoscale surface area of nanomaterials and the cell adhesive character of RGD peptide. In the long term, these results are envisaged for the construction of new biomaterials with other specific functionalizations for tissue engineering, drug delivery in 3D networks, and wound healing applications.

REFERENCES

- [1] P. Schexnailder, G. Schmidt. Nanocomposite polymer hydrogels. Colloid Polym. Sci. 2009, 287, 1.
- [2] K. Haraguchi. Nanocomposite hydrogels. Curr. Opin. Solid State Mater. Sci. **2007**, 11, 47.
- [3] R. Tutar, A. Motealleh, A. Khademhosseini, N. S. Kehr. Functional Nanomaterials on 2D Surfaces and in 3D Nanocomposite Hydrogels for Biomedical Applications. Adv. Func. Mater. 2019, 1904344.
- [4] K. Haraguchi, H. J. Li. Mechanical properties of nanocomposite hydrogels consisting of organic/inorganic networks and the effects of clay modification thereto. J. Network Polym. Jpn. 2004, 25, 81.
- [5] J. Mu, S. J. Zheng. Poly(N-isopropylacrylamide) nanocrosslinked by polyhedral oligomeric silsesquioxane: temperature-responsive behavior of hydrogels. Colloid Interface Sci. 2007, 307, 377.
- [6] Y. Kaneko, K. Noguchi, J. Kadokawa. Synthesis of temperature-responsive organic–inorganic hybrid hydrogel by free-radical polymerization of methacrylamide using water-soluble rigid polysiloxane having acryamido side-chains as a cross-linking agent. Polym. J. 2007, 39, 1078.
- [7] Y. Xiang, Z. Peng, D. Chen. A new polymer/clay nano-composite hydrogel with improved response rate and tensile mechanical properties. Eur. Polym. J. 2006, 42, 2125.
- [8] W. F. Lee, Y. C. Chen. Effect of intercalated hydrotalcite on swelling and mechanical behavior for poly(acrylicacid-co-N-isopropylacrylamide)/hydrotalcite nanocomposite hydrogels. J. Appl. Polym. Sci. 2005, 98, 1572.
- [9] S. H. Nair, K. C. Pawar, J. P. Jog, M. V. Badiger. Swelling and mechanical behavior of modified poly(vinyl alcohol)/laponite nanocomposite membranes. J. Appl. Polym. Sci. 2007, 103, 2896.
- [10] K. V. Durme, B. V. Mele, W. Loos, F. E. D. Introduction of silica into thermo-responsive poly(N-isopropyl acrylamide) hydrogels: A novel approach to improve response rates. Prez, Polymer 2005, 46, 9851.
- [11] W. C. Lin, W. Fan, A. Marcellan, D. Hourdet, C. Creton. Large Strain and Fracture Properties of Poly(dimethylacrylamide)/Silica Hybrid Hydrogels. Macromolecules, 2010, 43, 2554.
- [12] M. A. Cohen Stuart, Supramolecular perspectives in colloid science, Colloid Polym. Sci. 2008, 286, 855.
- [13] A. Motealleh, B. Celebi-Saltik, N. Ermis, S. Nowak, A. Khademhosseini, N. S. Kehr.
- 3D Printing of Step-Gradient Nanocomposite Hydrogels for Controlled Cell Migration.

Biofabrication, 2019, 11, 045015.

- [14] A. Motealleh, R. De Marco, N. S. Kehr. Stimuli-responsive Local Drug Molecule Delivery to Adhered Cells in a 3D Nanocomposite Scaffold. J. Mater. Chem. B., 2019, 7, 3716.
- [15] A. Motealleh, P. Dorri, A. H. Schäfer, N. S. Kehr. 3D Bioprinting of Triphasic

Nanocomposite Hydrogels and Scaffolds for Cell Adhesion and Migration.

- Biofabrication, 2019, 32, 035022.
- [16] A. Motealleh, N. S. Kehr. Janus Nanocomposite Hydrogels for Chirality-Dependent Cell Adhesion and Migration. ACS Appl. Mater. Interfaces. 2017, 9, 33674.
- [17] A. Motealleh, H. Hermes, J. Jose, N. S. Kehr. Chirality-Dependent Cell Adhesion and Enrichment in Janus Nanocomposite Hydrogels. Nanomedicine 2018, 14, 247.
- [18] N. S. Kehr, K. Riehemann. Controlled Cell Growth and Cell Migration in
- PMOs/Alginate Nanocomposite Hydrogels. Adv. Healthcare Mater. 2016, 5, 193.
- [19] N. S. Kehr, E. A.Prasetyanto, K. Benson, B. Ergün, A. Galstyan, H.-J. Galla.
- Periodic Mesoporous Organosilica-Based Nanocomposite Hydrogels as Three-
- Dimensional Scaffolds. Angew. Chem. Int. Ed., 2013, 52, 1156.
- [20] B. Hatton, K. Landskron, W. Whitnall, D. Perovic, G. A. Ozin. Past, Present, and Future of Periodic Mesoporous Organosilicas The PMOs. Acc. Chem. Res. 2005, 38, 305.
- [21] F. Hoffmann, M. Cornelius, J. Morell, M. Fröba. Silica-based mesoporous organic-inorganic hybrid materials. Angew. Chem. Int. Ed. 2006, 45, 3216.
- [22] W. J. Hunks, G. A. Ozin. Challenges and advances in the chemistry of periodic mesoporous organosilicas (PMOs). J. Mater. Chem. 2005, 15, 3716.
- [23] S. Inagaki, S. Guan, Y. Fukushima, T. Ohsuna, O. Terasaki. Novel Mesoporous Materials with a Uniform Distribution of Organic Groups and Inorganic Oxide in Their Frameworks. J. Am. Chem. Soc. 1999, 121, 9611.
- [24] T. Asefa, M. J. MacLachlan, N. Coombs, G. A. Ozin. Periodic mesoporous organosilicas with organic groups inside the channel walls. Nature 1999, 402, 867.
- [25] B. J. Melde, B. T. Holland, C. F. Blanford, A. Stein. Mesoporous Sieves with Unified Hybrid Inorganic/Organic Frameworks. Chem. Mater. 1999, 11, 3302.
- [26] L. L. Kerh, Z. Zhongxing, L. Jun. Supramolecular hydrogels based on
- cyclodextrin-polymer polypseudorotaxanes: materials design and hydrogel properties. Soft Matter, 2011, 7, 11290.
- [27] X. Liao, G. Chen, X. Liu, W. Chen, F. Chen, M. Jiang. Photoresponsive Pseudopolyrotaxane Hydrogels Based on Competition of Host–Guest Interactions. Angew. Chem. Int. Ed. 2010, 49, 4409.
- [28] J. P. Xiong, T. Stehle, R. G. Zhang, A. Joachimiak, M. Frech, S. L. Goodman, M. A. Aranout. Crystal Structure of the Extracellular Segment of Integrin $\alpha V \beta 3$ in Complex with an Arg-Gly-Asp Ligand. Science 2002, 296,151.
- [29] Y. W. Huang, M. Cambre, H. J. Lee. The Toxicity of Nanoparticles Depends on Multiple Molecular and Physicochemical Mechanisms. Int J Mol Sci. 2017, 18, 2702.